# Near Field Spectroscopic Investigation of Fluorescence Quenching by Charge Carriers in Pentacene-Doped Tetracene

**Jason D. McNeill,† Doo Young Kim, Zhonghua Yu, Donald B. O'Connor, and Paul F. Barbara***

*Center for Nano-Molecular Science and Technology, Department of Chemistry and Biochemistry, University of Texas at Austin, Austin, Texas 78712*

*Received: January 14, 2004; In Final Form: May 29, 2004*

The recently introduced technique of near field scanning optical microscopy (NSOM) with an electrically biased NSOM probe is applied in this paper to the study of exciton/polaron interactions in single crystals of the mixed organic semiconductor, tetracene doped with pentacene. As in the case of the previously investigated conjugated polymers, the injection of hole polarons induces extreme fluorescence quenching for tetracene/pentacene. However, the spectral selectivity, dynamics, and other features of the tetracene/pentacene data suggest a different mechanism than conjugated polymer for hole polaron interactions. The tetracene/pentacene mechanism is dominated by hole trapping by pentacene.

## Introduction

The relatively poorly understood interactions of excitons and polarons in organic materials can be important factors in key processes for device performance such as photoconductivity,[1,2] fluorescence quenching,[3,4] and polaron detrapping.[5] We recently developed a new technique for studying exciton/polaron interactions that is a modification of aperture near field scanning optical microscopy (NSOM) in which the NSOM probe is electrically biased.[6,7] In this approach, a sharpened, aluminum-coated optical fiber is maintained a few nanometers above the organic semiconductor using noncontact force feedback and serves both as a near field optical probe and as an electrode. Local charge carrier densities and dynamics are indirectly determined by carrier-induced near field fluorescence quenching in the near field region of the probe. Using this method, we previously determined both the fluorescence quenching volume for hole polarons in the conjugated polymer MEH−PPV and the hole polaron mobility.[7,8]

In this study, we apply the aforementioned near field microscopy techniques, and other techniques, to the organic semiconductor tetracene in order to determine the combined effects of energy transfer and charge trapping on fluorescence. We examine both pure tetracene crystals and tetracene crystals doped with varying amounts of pentacene. Tetracene doped with pentacene serves as a model system for organic semiconductors with a small concentration of low-energy traps. In agreement with the literature,[9] the fluorescence spectroscopy and lifetime measurements indicate efficient energy transfer from tetracene to pentacene. We find that application of a negative voltage bias to the near field probe causes quenching of the near field fluorescence. The amount of fluorescence quenching is highly dependent on the concentration of pentacene. For doped samples, a comparison of near field fluorescence spectra with and without a voltage bias indicates that pentacene cations quench tetracene fluorescence at a rate similar to that of neutral pentacene. The results are evidence that the combined effects of charge transfer and energy transfer to low-energy traps can be important factors in organic materials. The present results are consistent with our previous observation of large quenching volume for hole polarons in disordered polymer films.[8]

## Experimental Section

NSOM measurements were performed with a modified commercial near field scanning optical microscope (model Aurora 2 NSOM, ThermoMicroscopes, Inc.) that has been described in detail elsewhere.[8]

Tetracene single crystals were grown by horizontal physical vapor transport in a stream of hydrogen gas as described by Kloc and co-workers.[10] The resulting crystals consisted of plates a few millimeters in diameter and several microns thick. Crystals were mounted on a microscope cover glass that had been previously been coated with a transparent, conducting ITO layer using optical grade epoxy adhesive and cleaved to a thickness of 100−300 nm using an adhesive strip. The sample was electrically biased by attaching a programmable function generator to the coated fiber probe and the conducting ITO substrate. The electrical connection to the Al-coated fiber probe was made using a small amount of conducting epoxy, and the electrical connection to the conducting ITO substrate was made using silver paint. The transient photoluminescence response was recorded using a single photon avalanche photodiode and a counter−timer synchronized to the function generator. The near field fluorescence count rate was typically in the range of 10−20 kHz. Peak laser intensity (488 nm) at the sample was estimated at less than 0.2 W/cm$^2$. Transients were recorded for 5−20 min and summed to attain an acceptable signal-to-noise ratio. Photobleaching of the fluorescence was monitored and was typically less than 1% for a given NSOM measurement. Before each measurement, the sample was translated to reduce cumulative photobleaching. For each type of experiment, several runs were performed using different crystals and different NSOM probes. Similar results were obtained for each run.

* To whom correspondence should be addressed. E-mail: p.barbara@mail.utexas.edu.

† Present address: Department of Chemistry, Clemson University, Clemson, SC 29634.

10.1021/jp049823r CCC: $27.50 
Published on Web 07/07/2004

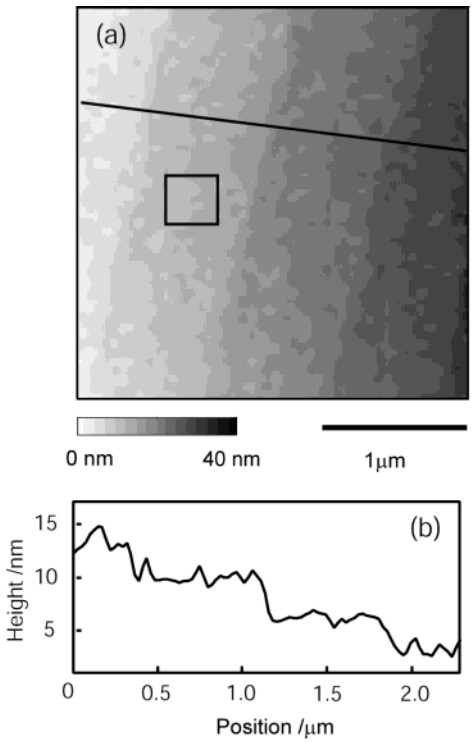


**Figure 1.** (a) Topographical image of tetracene single crystal showing a series of molecular steps. RMS roughness in the rectangular area is ~1 nm. (b) Height profile along a line drawn in (a).

Photoluminescence spectra were recorded by liquid nitrogen-cooled CCD spectrometer with and without a pulsed electric field (90% duty cycle). Fluorescence decays were obtained by time-correlated single photon counting (TCSPC) with 488 nm excitation pulses ($\Delta t$ ~200 fs, repetition rate 3.8 MHz) from a mode-locked Ti−sapphire laser system (Coherent Mira 900, Coherent Pulse Picker model 9200, Inrad SHG/THG model 5-050) and a Hamamatsu R3809U-50 microchannel plate PMT. Emission was collected at 90° with respect to the incident excitation axis through a Glan-Taylor polarizer set at the "magic angle" of 54.7°. The emission wavelength was selected using 10 nm width band-pass filters. The emission decay curves were fit to a sum of exponential decays convoluted with the instrument response (~50 ps fwhm).

## Results

**Crystal Morphology.** Mounted and cleaved crystals were platelets typically several tens of microns across and ~100−250 nm thick. Images of the topography indicated large, flat regions with occasional molecular step edges (see Figure 1). The distance between molecular step edges varied from crystal to crystal between 0.5 $\mu$m and tens of microns. The step depth in these images varies between 1 and 3 molecular layers with a depth of the shallowest steps of 1.2 nm, in agreement with literature results.[11] NSOM images of the pentacene fluorescence indicate that pentacene concentration is uniform over the 100 nm to 5 $\mu$m length scale (Figure 2). The near field fluorescence images demonstrated that the pentacene did not segregate appreciably at step edges.

**Near Field Fluorescence Spectra.** Figure 3 portrays fluorescence spectra excited by a NSOM tip at zero electrical bias. Spectra are shown for pure tetracene and tetracene doped with a series of pentacene concentrations. The concentration was estimated by comparison to literature spectra.[9,12] The relatively high intensity of the pentacene fluorescence given the low

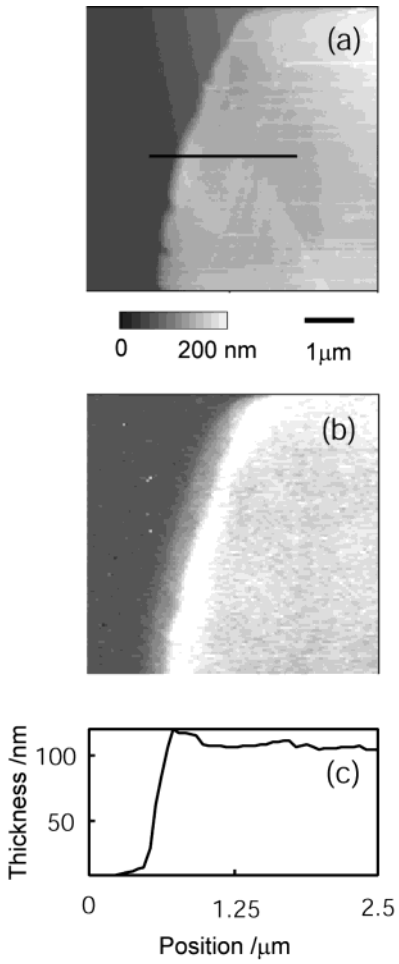


**Figure 2.** (a) Topography and (b) NSOM image of a tetracene single-crystal edge and (c) thickness profile along a line drawn in (a).

pentacene concentration is due to efficient energy transfer from the tetracene (donor) to the pentacene (acceptor). A Förster radius of 1 nm is reported in the literature.[12] The apparent energy transfer length, however, is much larger due to exciton diffusion in tetracene. The exciton diffusion length in pure tetracene is estimated at between 12 and 29 nm.[13] At 20 ppm of pentacene, the average distance between a donor and the nearest acceptor is 14 nm (assuming random acceptor positions).

**Fluorescence Lifetime.** Figure 4 illustrates fluorescence intensity vs time traces for pure and doped tetracene (100 ppm pentacene). The results were obtained with ~5 $\mu$m thick crystals. The pure tetracene fluorescence transient ($\lambda$ = 540 nm) has a fast component with a time constant of 160 ps, a slow component with a time constant of 1070 ps, and a rising component with a time constant of 24 ps. The time constant of the fast component is similar to the singlet lifetime obtained by transient absorption spectroscopy.[14] The slow component, which is probably due to tetracene−tetracene energy transfer, is consistent with results from the literature.[15] The rising component is assigned to diffusion of excitons generated in the interior of the crystal.[12,15] The addition of 100 ppm of pentacene decreases the tetracene singlet lifetime by 50%, demonstrating substantial energy transfer. The tetracene fluorescence of the doped sample lacks a rising component, indicating a lower energy diffusion length in doped tetracene.

**Charge Carrier-Induced Fluorescence Quenching.** The application of a sequence of voltage pulses to the aluminum coating on the NSOM probe resulted in a modulation of the fluorescence intensity, shown in Figure 5. The results are

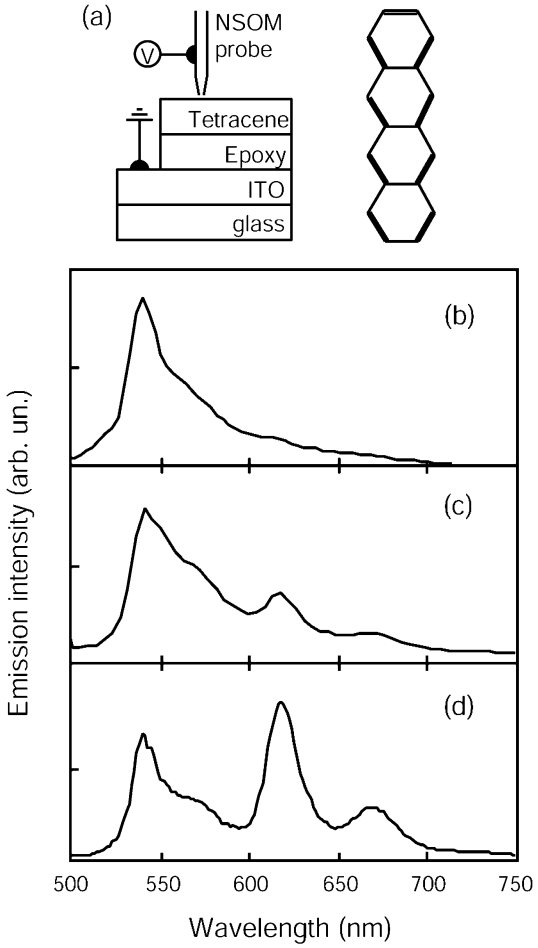


**Figure 3.** (a) Sample and probe with connection to function generator for application of electrical pulses. Photoluminescence spectra of (b) pure tetracene crystal, (c) tetracene crystal doped with low concentration of pentacene (~5 ppm), and (d) tetracene doped with high concentration of pentacene (~50 ppm).

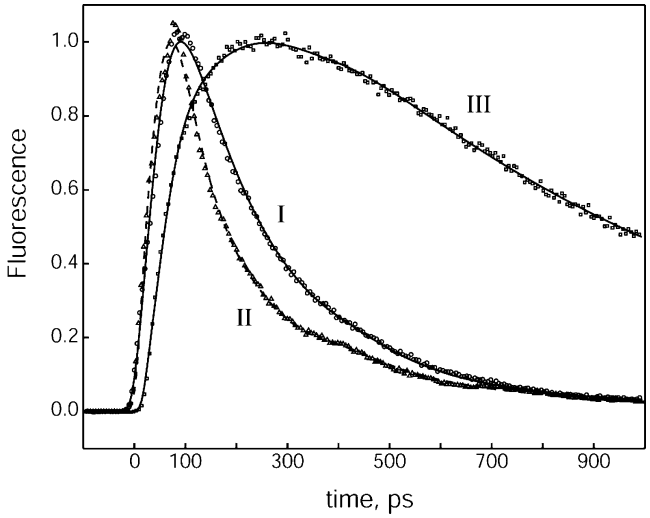


**Figure 4.** Fluorescence lifetime data for pure and doped tetracene (100−200 ppm pentacene). Excitation is at 488 nm. Circles (a) indicate fluorescence lifetime data for pure tetracene (540 nm), triangles (b) indicate lifetime data for doped tetracene (540 nm), and squares (c) indicate pentacene fluorescence (620 nm).

qualitatively similar to results of analogous experiments on conjugated polymer films.[8] Application of a negative bias to the probe causes a decrease in fluorescence intensity that we attribute to fluorescence quenching by hole polarons held in

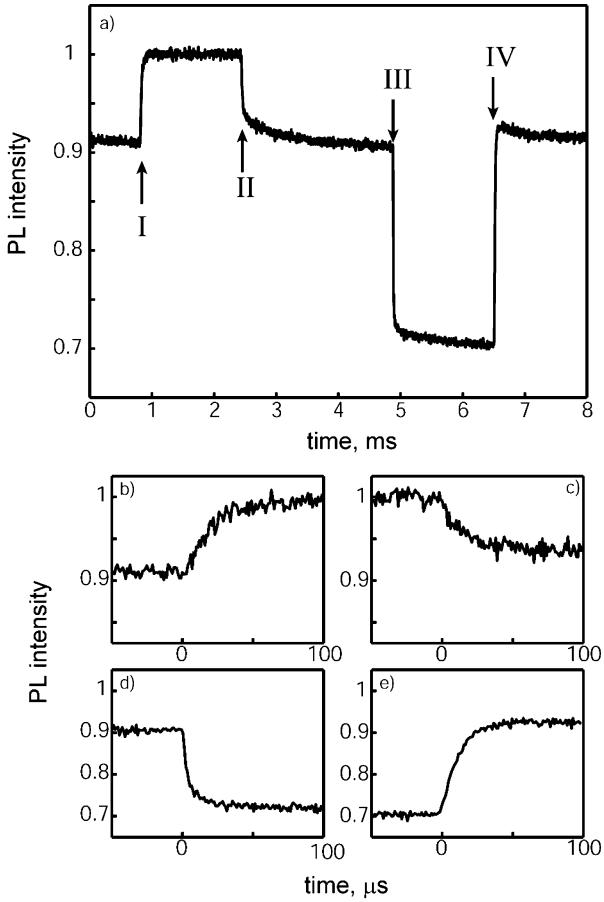


**Figure 5.** Panel (a) is the transient response of doped tetracene fluorescence for an 8 ms cycle with 1 $\mu$s resolution. The arrows indicate the parts of the trace corresponding to panels (b)−(e). Panels (b)−(e) show the response within the first 100 $\mu$s upon application or removal of electrical bias.

the attractive potential well of the biased tip, while the application of a positive bias caused an increase in the fluorescence signal. The amount of fluorescence increase upon application of a positive bias to the probe depends on laser power and doping concentration. We attribute the increase in fluorescence upon application of a positive bias to electrostatic repulsion of hole polarons from the vicinity of the NSOM tip. There is no increase in fluorescence upon application of a positive bias for pure tetracene. This is consistent with the expectation that the steady-state hole concentration should be lower in the pure semiconductor, tetracene, than in the doped crystals, since doped semiconductors usually have greater photoconductivity.[16]

Figure 6 shows how the steady-state fluorescence spectrum depends on electrical bias for samples with different levels of pentacene doping. Only the pentacene portion of the spectrum (peaked near 620 nm) is affected by changes in the electrical bias. For pure tetracene, no change in the spectrum was evident. The spectra strongly suggest that hole polarons are trapped by pentacene. The quenching is completely reversible upon reversal of the electrical bias, indicating reversible oxidation of pentacene. The quenching ratio, $Q = 1 - f/f_0$, decreases with increasing pentacene concentration. A quenching of 80% of the pentacene fluorescence is observed for tetracene samples doped with approximately 10 ppm of pentacene upon application of −10 V to the probe, while a quenching ratio of 20% is observed for tetracene doped with approximately 50 ppm. The application of a negative voltage bias causes a significant reduction in the intensity of the (pentacene) acceptor fluorescence without a

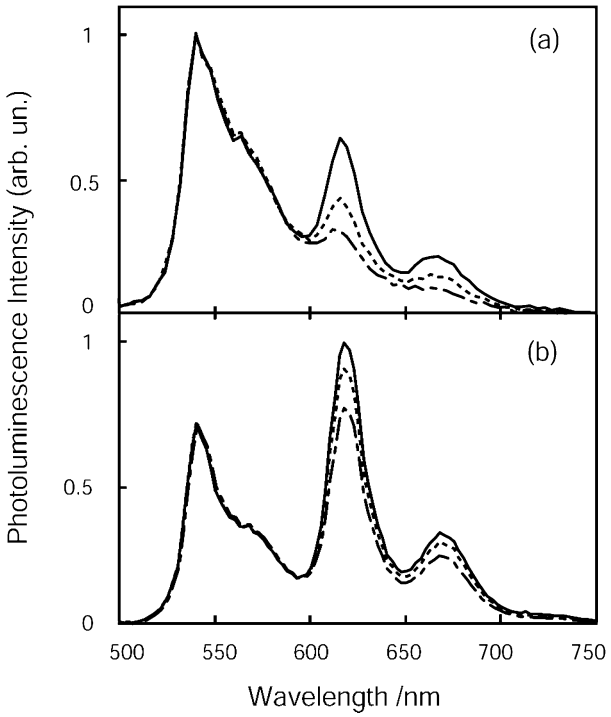


**Figure 6.** Pentacene concentration dependence of photoluminescence spectra (a) low concentration (~5 ppm) and (b) large concentration (~50 ppm) of pentacene at 10 V (solid), 0 V (dotted), and −10 V (dashed) applied to the tip.

concomitant increase in the tetracene fluorescence. This behavior was observed for several samples and for varying concentrations of pentacene.

Figure 5 shows that the field induced fluorescence dynamics occurs on a distribution of time scales ranging from dominant effects on the microsecond time scale to more subtle effects on the millisecond, and even second (not shown), scale. The microsecond time scale processes appear to be associated with hole polaron drift in response to the intense $E$ field of the near field probe, i.e., ~0.1−0.5 MV/cm. A field-induced drift over the 100−400 nm region of the probe implies a hole mobility of $\sim 10^{-4}-10^{-5}$ cm$^2$/(V s). This value is small compared to reports of tetracene holes in pure crystals but is not surprising since the holes are effectively trapped in pentacene and hole conduction requires detrapping.

The slower dynamical processes in Figure 5 are reminiscent, though much less prevalent than analogous data for conjugated polymers. On the basis of recent current−voltage experiments on organic devices,[17] these slower processes are probably associated with deep hole traps, which are a characteristic property of organic semiconductors.[18,19] Hole trapping by reduction products of atmospheric impurities (e.g., $^-$OH) may be another factor since these samples are exposed to the atmosphere.[20−22]

Assuming static quenching of the pentacene fluorescence by hole polarons, the decrease in fluorescence intensity for a negative bias applied to the probe can be modeled using the Stern−Volmer equation, $F_0/F = 1 + Kn_h$, where $F_0/F$ is the ratio of initial and quenched fluorescence intensities, $K$ is the quenching ratio, and $n_h$ is the concentration of holes.[23] Figure 7 contains an approximate fit of the fluorescence intensity to a Stern−Volmer model, assuming the concentration of cation quenchers is proportional to the voltage bias for negative biases applied to the probe and that a fraction of the fluorescence signal (75%) is not subject to quenching.

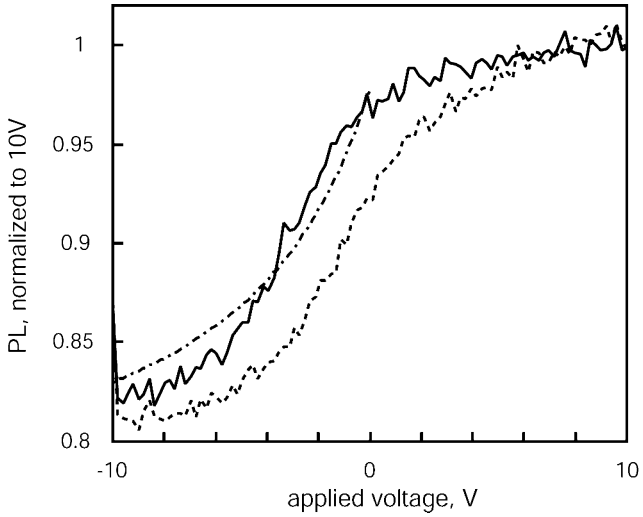


**Figure 7.** Voltage dependence of the photoluminescence intensity measured with the doped tetracene (where Figure 3d was measured). The solid lines indicate measurements performed while the sample was scanning at a rate of 500 nm/s. The dotted lines indicate measurements performed while the sample was held stationary. The dashed line indicates the predicted fluorescence intensity assuming a Stern−Volmer model.

## Discussion

The general trends of data are consistent with simple filling of pentacene sites with pentacene holes as being the dominant mechanism of fluorescence quenching. The fluorescence yields of holes are negligible, so only pentacene and tetracene excitons are significant contributors to fluorescence. The decrease in fractional fluorescence yield with increasing pentacene doping supports the hole filling model. It furthermore suggests that pentacene holes do not effectively quench the pentacene emission of an adjacent pentacene site, which is not surprising considering the low concentration of pentacene.

**Quenching Processes.** Tetracene offers a wide variety of processes involving excited species.[24] Tetracene doped with pentacene has previously been studied using time-resolved fluorescence spectroscopy.[12] We first discuss the following processes describing fluorescence and energy transfer in tetracene doped with pentacene

$$T + h\nu \rightarrow T_S \quad (1a)$$

$$T_S \rightarrow T + h\nu \quad (1b)$$

$$T_S + T \rightarrow T + T_S \quad (1c)$$

$$T_S + P \rightarrow T + P_S \quad (1d)$$

$$P_S \rightarrow P + h\nu \quad (1e)$$

$$T_S + P^+ \rightarrow T + P^+ \quad (1f)$$

where (1a) describes optical absorption by tetracene, (1b) describes tetracene fluorescence, (1c) describes hopping of tetracene singlet excitons from one molecule to another, (1d) describes energy transfer from tetracene to pentacene, (1e) describes pentacene fluorescence, and (1f) describes quenching of tetracene singlet excitons by pentacene cations. The higher position of the HOMO level in pentacene as compared to tetracene strongly suggests that hole polarons can be trapped on pentacene, generating pentacene cations.

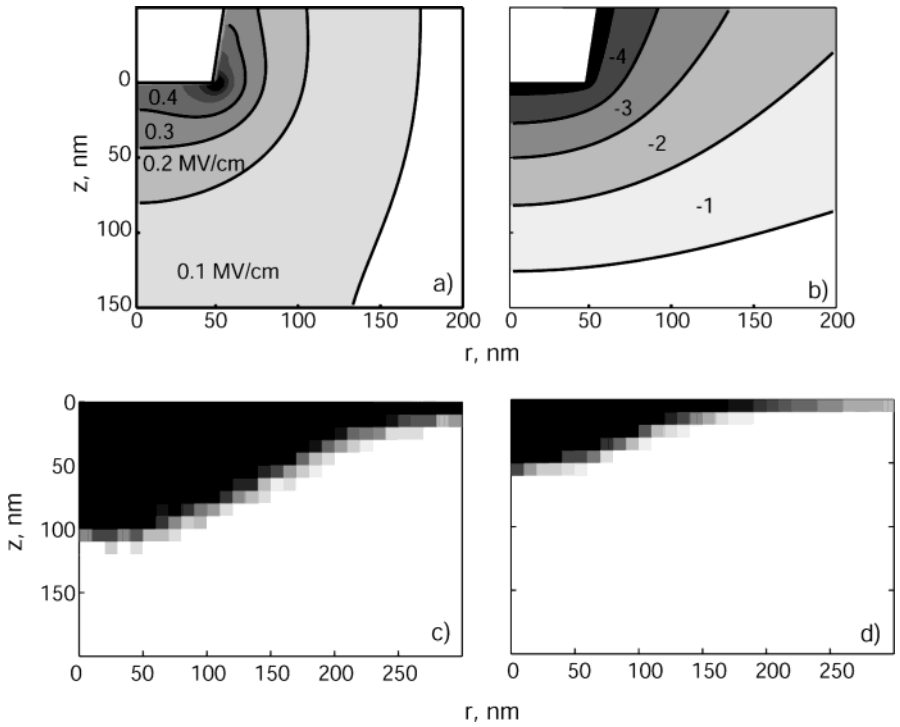


**Figure 8.** Panels (a) and (b) depict the electric field and electric potential, respectively, for an electrically biased NSOM probe. Panels (c) and (d) depict the distribution of charge carriers assuming a 20 ppm (c) and 80 ppm (d) site density.

A separate issue, however, is whether pentacene holes effectively quench tetracene excitons. As shown above in a highly doped tetracene/pentacene sample at zero bias, the exciton lifetime is ~50% shorter than pure tetracene, implying a tetracene to pentacene energy transfer efficiency of ~50%. Thus, the observation that substantial pentacene site filling by holes at high bias does not alter the tetracene fluorescence intensity actually implies that neutral pentacene sites and hole-filled sites have approximately equal propensity for quenching singlet excitons in tetracene.

Quantitative information on the fluorescence quenching process is available in combined analyses of the lifetime and yield data. Assuming a literature value for the fluorescence quantum yield of pure tetracene of 15%,[14] comparing the tetracene lifetimes for pure vs doped tetracene (100 ppm) yields a tetracene to pentacene energy transfer rate of approximately 240 $ps^{-1}$ and an energy transfer efficiency of approximately 40%. If we assume no quenching by pentacene cations (i.e., hole trapping merely reduces the concentration of neutral pentacene), a decrease of 10% in the pentacene fluorescence yield caused by hole trapping should yield an increase of 4% in the tetracene fluorescence yield. According to the comparison between spectra with and without holes, the increase in tetracene fluorescence associated with charge trapping at pentacene is less than 1%. This leaves two possibilities: either the quenching volume of pentacene cations is similar to that of neutral pentacene or quenching of tetracene singlets by tetracene cations compensates for the lifetime increase associated with the lower pentacene (neutral) concentration. According to our measurements of fluorescence quenching by cations in pure tetracene, the quenching efficiency is several times lower than the amount required to compensate for the lower concentration of pentacene neutral. If we assume the rate of quenching by tetracene cations is the same or lower in doped samples, then quenching by tetracene cations is not sufficient to explain the intensity of tetracene fluorescence in the presence of pentacene cations. Therefore, we conclude that pentacene cations quench tetracene fluorescence and that the quenching volume for the cation is approximately the same as that of neutral pentacene.

Here we discuss three possible quenching mechanisms involving the pentacene cation: Förster transfer, Dexter transfer, and charge transfer. We assume that quenching is diffusion-controlled, with a quenching rate given by the Smoluchowski relation,[12,25] $k = 4\pi cDR$, where $c$ is the concentration, $D$ is the diffusion constant, and $R$ is the interaction radius. In general, the interaction radius depends on the nature of the interaction and its characteristic length scale. For Förster transfer, the characteristic length scale is related to the Förster radius, which depends on the overlap between donor emission and acceptor absorption. However, little is known about the absorption spectrum of pentacene cation in a tetracene matrix. According to the studies of pentacene cations in a noble gas matrix, there are bands at 426, 842, and 954 nm.[26] None of these bands have appreciable overlap with the tetracene fluorescence bands from 540 to 650 nm, suggesting that Förster transfer is not involved. However, wave function overlap between the pentacene cation and neighboring tetracene molecules could shift these bands, thus improving overlap. Charge transfer or Dexter transfer from tetracene singlet excitons to pentacene cations could also contribute to quenching. However, one would expect that the interaction length and therefore the rate of quenching would be much lower for Dexter transfer and charge transfer as compared to Förster transfer, since Dexter and charge transfer processes involve wave function overlap and are restricted to nearest neighbors. We must conclude that either the interaction radius $R$ is similar for $T \rightarrow P$ and for $T \rightarrow P^+$ or that contributions from other processes such as quenching by tetracene cations have been underestimated. One possible explanation for the apparently large interaction length for the pentacene cation is the presence of exciton traps near the dopant molecule arising from random dislocations or local distortion of the crystal lattice induced by the presence of the dopant molecule.[12,27] Such traps could act as intermediates in the energy transfer process, in which case the energy transfer rate would be determined by

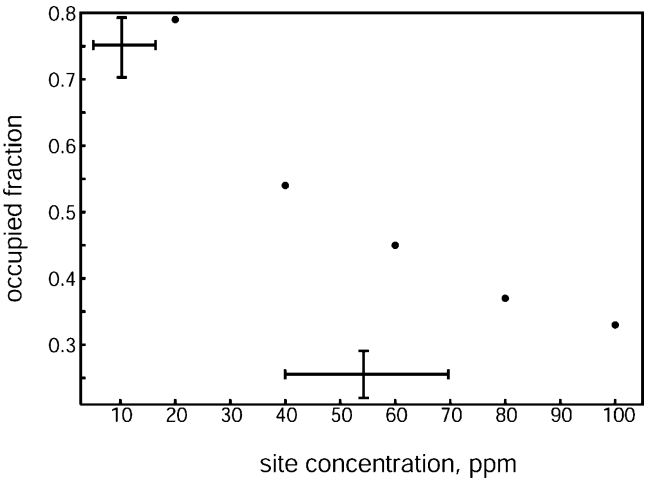


**Figure 9.** Fraction of pentacene sites within the near field probe volume occupied by hole polarons, for −10 V applied to tip. Crosses denote values derived from near field spectroscopy results, and circles denote results of simulation.

the radius for energy transfer to tetracene traps. Additional studies are required to determine the exact quenching mechanism for pentacene cations.

**Spatial Distribution of Occupied Traps**. Under the asymmetric electrode geometry of electrical measurements with the near field probe, it is necessary to consider the configuration of the electric field, the distribution of charge carriers, and the volume overlap of the carriers with the near field illumination volume in order to model the dependence of fluorescence quenching on voltage and concentration of dopant. The picture developed previously is that the electrically biased near field probe acts as an electrostatic trap for photogenerated cations.[8] Here we present the results of additional calculations to estimate the distribution of charge carriers under the near field probe. The electrostatic potential around a near field probe was calculated by numerically solving Poisson's equation using the multigrid relaxation method for an idealized geometry in cylindrical coordinates.[28] The calculated potential and the electric field strength are shown in Figure 8. The maximum field strength is ∼1 MV/cm while the average field strength within the probe volume is 0.2−0.4 MV/cm. The charge distribution under the probe was calculated as follows. It was assumed that the cations reside on pentacene sites randomly distributed in the crystal lattice. For a bias of −10 V applied to the probe, the potential well due to the probe can hold approximately 900 positive charge carriers. The charges were placed within the slab and the total energy was minimized, yielding the charge densities shown in Figure 8. The calculated charge density profile has appreciable overlap with the near field illumination volume.

To model the effect of dopant concentration and bias voltage on the near field fluorescence spectrum, we calculated the fraction of occupied pentacene sites within the near field probe volume using the same model, for a range of dopant concentrations and a tip bias of −10 V. The near field probe volume is defined by the near field illumination profile, the optical absorption coefficient of the sample, the thickness of the sample, and the collection volume of the collection objective. The probe volume was assumed to be a cylinder with a diameter of 100 nm and a height of 150 nm. The fraction of occupied pentacene sites within the probe volume was calculated for a −10 V bias over the range of 10−100 ppm and compared to the experimental results for pentacene quenching for a bias of −10 V (Figure 9). The results of the calculation qualitatively agree with the change in pentacene fluorescence intensity observed for a given concentration upon application of a −10 V bias to the tip. This provides further indication that the fluorescence quenching upon application of a voltage bias to the tip is due to charge trapping at pentacene sites within the potential well provided by the near field probe and that the calculated charge distribution (and its dependence on pentacene concentration) is qualitatively correct. This also provides indication that the number of charges under the tip is approximately proportional to voltage, in agreement with the Stern−Volmer analysis in Figure 7. In summary, we conclude that holes primarily reside on pentacene sites, the distribution of charge density is determined by the dopant density, and the total number of charges under the probe is proportional to voltage, according to the potential well provided by the biased near field probe.

## Summary and Conclusions

We have described the results of a set of experimental investigations into charge carrier-induced fluorescence quenching in tetracene single crystals molecularly doped with pentacene. A large fluorescence quenching volume was determined for pentacene cations embedded in a crystalline tetracene host. The observed quenching volume was much larger than for charge carriers in pure tetracene and was similar to that of the neutral pentacene dopant. The exact quenching mechanism is not known, but the mechanism could involve exciton traps near dopant sites in the crystal lattice. The results provide a strong indication of the importance of energetic disorder in quenching by cations in molecular semiconductors. The observed large fluorescence quenching volume for dopant cations have implications for organic light-emitting devices based on disordered or doped materials.[29] The dependence of the fluorescence spectrum on voltage and dopant concentration is consistent with charge trapping at pentacene sites within the potential well presented by the electrically biased near field probe.

**Acknowledgment.** We gratefully acknowledge the Welch Foundation and the National Science Foundation for support of this research.

## References and Notes

(1) Bassler, H. *Adv. Mater.* **1993**, *5*, 662.
(2) Kalinowski, J.; Stampor, W.; Di Marco, P. *J. Electrochem. Soc.* **1996**, *143*, 315.
(3) Tasch, S.; Kranzelbinder, G.; Leising, G.; Scherf, U. *Phys. Rev. B* **1997**, *55*, 5079.
(4) Deussen, M.; Scheidler, M.; Bassler, H. *Synth. Met.* **1995**, *73*, 123.
(5) Liu, C. Y.; Pan, H. L.; Fox, M. A.; Bard, A. J. *Chem. Mater.* **1997**, *9*, 1422.
(6) McNeill, J. D.; O'Connor, D.; Barbara, P. F. *J. Chem. Phys.* **2000**, *112*, 7811.
(7) McNeill, J. D.; O'Connor, D. B.; Adams, D. M.; Kämmer, S. B.; Barbara, P. F. *J. Phys. Chem. B* **2001**, *105*, 76.
(8) McNeill, J. D.; Barbara, P. F. *J. Phys. Chem. B* **2002**, *106*, 4632.
(9) Geacintov, N. E.; Burgos, J.; Pope, M.; Strom, C. *Chem. Phys. Lett.* **1971**, *11*, 504.
(10) Kloc, C.; Simpkins, P. G.; Siegrist, T.; Laudise, R. A. *J. Cryst. Growth* **1997**, *182*, 416.
(11) Overney, R. M.; Howald, L.; Frommer, J.; Meyer, E.; Guntherodt, H.-J. *J. Chem. Phys.* **1991**, *94*, 8441.
(12) Campillo, A. J.; Shapiro, S. L.; Swenberg, C. E. *Chem. Phys. Lett.* **1977**, *52*, 11.
(13) Matsui, A. *J. Opt. Soc. Am. B* **1990**, 1615.
(14) Frolov, S. V.; Kloc, C.; Schon, J. H.; Batlogg, B. *Chem. Phys. Lett.* **2001**, *334*, 65.
(15) Campillo, A. J.; Hyer, R. C.; Shapiro, S. L.; Swenberg, C. E. *Chem. Phys. Lett.* **1977**, *48*, 495.
(16) Barth, S.; Bassler, H.; Rost, H.; Horhold, H. H. *Phys. Rev. B* **1997**, *56*, 3844.

(17) Bozano, L.; Carter, S. A.; Scott, J. C.; Malliaras, G. G.; Brock, P. J. *Appl. Phys. Lett.* **1999**, *74*, 1132.

(18) Antoniadis, H.; Abkowitz, M. A.; Hsieh, B. R. *Appl. Phys. Lett.* **1994**, *65*, 2030.

(19) Bulovic, V.; Forrest, S. R. *Chem. Phys.* **1996**, *210*, 13.

(20) Papadimitrakopolous, F.; Konstandinidis, K.; Miller, T.; Opila, R.; Chandross, E.; Galvin, M. *Chem. Mater.* **1994**, *6*, 1563.

(21) Harrison, M. G.; Gruner, J.; Spencer, G. C. W. *Phys. Rev. B* **1997**, *55*, 7831.

(22) Silinsh, E. A.; Capek, V. *Organic Molecular Crystals: Interaction, Localization, and Transport Phenomena*; AIP Press: New York, 1994.

(23) Lakowicz, J. R. *Principles of Fluorescence Spectroscopy*; Plenum Press: New York, 1983.

(24) Pope, M.; Swenberg, C. E. *Electronic Processes in Organic Crystals*; Clarendon: Oxford, 1982.

(25) Kenkre, V. M.; Parris, P. E.; Schmid, D. *Phys. Rev. B* **1985**, *32*, 4946.

(26) Szczepanski, J.; Wehlburg, C.; Vala, M. *Chem. Phys. Lett.* **1995**, *232*, 221.

(27) Birks, J. B. *Photophysics of Aromatic Molecules*; Wiley-Interscience: New York, 1970.

(28) Press, W. H.; Teukolsky, S. A.; Vetterling, W. T.; Flannery, B. P. *Numerical Recipes in C*; Cambridge University Press: Cambridge, 1988.

(29) Adachi, C.; Baldo, M. A.; Thompson, M. E.; Forrest, S. R. *J. Appl. Phys.* **2001**, *90*, 5048.